

Development of an API 5L X-70 Grade Steel for Sour Gas Resistance Pipeline Application

R. Mendoza, J. Huante, V. Camacho, O. Alvarez-Fregoso, and J.A. Juarez-Islas

(Submitted 30 October 1998; in revised form 25 May 1999)

An API 5L X-70 grade steel for large diameter pipeline application with sour gas resistance was developed by electric arc furnace processing, furnace ladle treatment, vacuum degassing, ladle treatment, and continuous casting, followed by three different controlled rolling schedules and air cooling or accelerated cooling. Mechanical properties equivalent to those of an API 5L X-70 grade steel were achieved in slabs with content ranges from 0.25 to 0.37 wt% C, 1.31 to 1.53 wt% Mn, 0.082 to 0.095 wt% Nb, and 0.008 to 0.015 wt% Ti. The slabs were processed by using a controlled rolled and accelerated cooling schedule.

Keywords API X-70 grade steel, casting, hot rolling, mechanical properties, microstructure

1. Introduction

The purpose of this article is to report the steelmaking and thermomechanical processing route used to obtain a 5L X-70 grade steel for sour gas resistance pipeline application.

Recent developments in Mexican pellet workshops, including direct reduction, steelmaking, vacuum degassing, ladle refining/calcium treatment, and continuous casting technology, have led to the production of steels containing microalloying constituents, which are controlled in parts per million. Great improvements in steelmaking practices have allowed improved alloy composition through production of steels with low interstitial element contents (carbon, C, and nitrogen, N), low sulfur contents (to reduce hydrogen-induced cracking), and low phosphorus levels (to lower the hardening tendency of segregated regions) (Ref 1). The resultant steels present ferrite grains with very low levels of nonmetallic inclusions. Sulfide-shape control permits improved notch toughness and resistance to sour gas degradation of pipelines.

One of the most relevant processing applications of thermomechanically rolled steels is plate/skelp for large diameter pipes, where grade X-70 has become the major applied steel grade (Ref 2). Several studies have been carried out in order to correlate niobium (Nb) contents with controlled rolling schedules (Ref 3, 4) plus the effect of accelerated cooling (Ref 5) in order to achieve two goals, that is, sour gas resistance and X-80 properties (Ref 2-4).

Hot rolling schedules applied to X-70 grade steel have been carried out in order to maintain a high initial temperature so that finishing roughing passes are completed in the fully austenitic

temperature range and so that dissolution of carbides, nitrides, or carbonitrides that need to be precipitated at some later stage of processing is ensured (Ref 6).

When steel is deformed at high temperatures, recrystallization is complete before subsequent deformation steps. Following recrystallization, grain growth can occur, depending on time, temperature, and amount of precipitates. As the temperatures decrease, recrystallization can be partially or totally suppressed, so that grain flattening and strain accumulation occur. At very low temperatures, the deformation is extended to the austenite plus ferrite region, and both phases are deformed. Precipitate compounds appear as the temperature of steel decreases, supersaturating the austenite so that precipitate nucleation occurs and is followed by particle growth (Ref 7). Accelerated cooling practices after finish rolling ensure strength properties by controlling temperature and microstructure (Ref 8) with the objective of forcing deformation and recrystallization to lower temperatures, thereby maximizing austenite grain refinement (Ref 9). Of course, the choice of technique used depends on the microalloying system in use and the particular product form and manufacturing facility available.

2. Experimental Procedure

The Imexsa steelmaking route (Ispat Mexicana, S.A. de C.V., Lazaro Cardenas, Michoacan, Mexico) for producing an API 5L X-70 grade steel for sour gas pipeline application consisted of charging 100% high metallization-grade sponge iron into the electric arc furnace; during the melting operation, calcium hydroxide ($\text{Ca}(\text{OH})_2$), coke, and oxygen were added. After melting and deslagging, the steel was poured from the electric arc furnace to a ladle furnace. Immediately afterward $\text{Ca}(\text{OH})_2$, FeMn, and FeNi were added. Then, the steel in the ladle furnace was sent to a vacuum degassing unit; during this operation, synthetic slag (aluminum, Al, and CaF_2) was added. After degassing, additions of copper (Cu), CaF_2 , FeCr, $\text{Ca}(\text{OH})_2$, FeNb, FeSi, FeMn, and Al were carried out under argon bubbling. After these additions, the 200 tons of steel were continuously cast. The resulting slabs showed dimensions of 0.80 by 1.20 by 0.25 m. Table 1 shows the final chemical com-

R. Mendoza and J. Huante, Ispat Mexicana, S.A. de C.V. Aseguramiento de la Calidad, Fco. J. Mújica No 1B, Cd. Lazaro Cardenas, Michoacan, Mexico; V. Camacho, Productora Mexicana de Tubería, Boulevard de las Bahías S/N, Cd. Lazaro Cardenas, Michoacan, Mexico; and O. Alvarez-Fregoso and J.A. Juarez-Islas, Departamento de Materiales Metalicos y Ceramicos, Instituto de Investigaciones en Materiales-UNAM, Circuito exterior S/N, Cd. Universitaria, 04510, Mexico, D.F., Mexico. Contact e-mail: julioalb@servidor.unam.mx.

position of steels for heats 9,722,417; 9,722,416; 9,712,173; 9,722,425; 9,712,182; 9,722,418; and 9,712,174.

During thermomechanical processing, slabs were soaked at a temperature of 1250 ± 6 °C (γ region) for approximately 6 h under a protective atmosphere and then rough rolled, achieving at the end of this rolling operation $\approx 66\%$ of total reduction (in approximately 9 to 11 steps) on the 0.25 m slab. The final rough rolling temperature was ≈ 1020 °C (γ region), and the slab thickness was ≈ 8.0 cm. Then, the hot rough rolled slab was sent to the finishing rolling mill. At this stage, if the rolling temperature was higher than approximately 1020 °C, then the rough

rolled slab was left to achieve that temperature. The holding time was between 90 to 210 s.

The initial rolling temperature at this stage on 20 slabs was ≈ 1020 °C, and the initial slab thickness was ≈ 0.080 m. The finishing rolling operation was carried out according to one of the following three schedules:

- *Rolling schedule No. 1:* A controlled rolling procedure for three slabs (9,712,173; 9,722,416; and 9,722,417) with low manganese (Mn) contents (1.28, 1.33, and 1.33 wt%, respectively) and three slabs (9,722,418; 9,712,182; and

Table 1 Chemical composition of steel grade API 5L X-70

Cast-slab	Grade	Composition, wt%										
		C	Mn	Si	S	Al	Nb	Cu	Cr	Ni	N ₂	Ti
9,722,417-253	G954	0.025	1.33	0.180	0.002	0.028	0.095	0.280	0.282	0.168	0.003	0.008
9,722,416-252	G954	0.020	1.31	0.160	0.002	0.028	0.092	0.280	0.264	0.183	0.003	0.008
9,712,173-207	G954	0.030	1.28	0.180	0.001	0.037	0.090	0.262	0.272	0.165	0.005	0.008
9,722,425-253	G974	0.030	1.53	0.170	0.003	0.032	0.092	0.280	0.289	0.159	0.004	0.011
9,712,182-205	G974	0.037	1.51	0.140	0.002	0.032	0.092	0.27	0.266	0.157	0.004	0.010
9,722,418-109	G964	0.031	1.49	0.210	0.001	0.028	0.082	0.270	0.281	0.162	0.004	0.009
9,722,417-203	G954	0.025	1.33	0.180	0.002	0.028	0.095	0.280	0.282	0.168	0.003	0.008
9,722,416-202	G954	0.020	1.31	0.160	0.002	0.028	0.092	0.280	0.264	0.183	0.003	0.008
9,722,416-203	G954	0.020	1.31	0.160	0.002	0.028	0.092	0.280	0.264	0.183	0.003	0.008
9,722,425-203	G974	0.030	1.53	0.170	0.003	0.032	0.092	0.280	0.289	0.159	0.004	0.011
9,712,182-204	G974	0.037	1.51	0.140	0.002	0.032	0.092	0.270	0.266	0.157	0.004	0.010
9,722,418-107	G964	0.031	1.49	0.210	0.001	0.028	0.082	0.270	0.281	0.162	0.004	0.009
9,722,417-205	G954	0.025	1.33	0.180	0.002	0.028	0.095	0.280	0.282	0.168	0.003	0.008
9,722,417-255	G954	0.025	1.33	0.180	0.002	0.028	0.095	0.280	0.282	0.168	0.003	0.008
9,722,416-205	G954	0.020	1.31	0.160	0.002	0.028	0.092	0.280	0.264	0.183	0.003	0.008
9,722,416-255	G954	0.020	1.31	0.160	0.002	0.028	0.092	0.280	0.264	0.183	0.003	0.008
9,722,425-204	G974	0.030	1.53	0.170	0.003	0.032	0.092	0.280	0.289	0.159	0.004	0.011
9,712,174-106	G964	0.035	1.48	0.190	0.002	0.026	0.099	0.259	0.269	0.158	0.005	0.015
9,712,182-206	G974	0.037	1.51	0.140	0.002	0.032	0.092	0.270	0.266	0.157	0.004	0.010
9,722,418-104	G964	0.031	1.49	0.210	0.001	0.028	0.082	0.270	0.281	0.162	0.004	0.009

P is present in the range between 0.014 and 0.015. Mo is zero except for the cast 9,712,163 (0.001 wt%), and B is zero except for the cast 9,722,416 (0.0001 wt%).

Table 2 Final rolling schedules applied to Imexsa slabs

Cast-slab identification	Mn, wt%	Final rolling temperature(a), °C	Cooling
9,722,417-253	1.33	835	Air until RT is reached
9,722,416-252	1.31	835	Air until RT is reached
9,712,173-207	1.28	835	Air until RT is reached
9,722,425-253	1.53	835	Air until RT is reached
9,712,182-205	1.51	835	Air until RT is reached
9,722,418-109	1.49	835	Air until RT is reached
9,722,417-203	1.33	795	Air until RT is reached
9,722,416-202	1.31	795	Air until RT is reached
9,722,416-203	1.31	795	Air until RT is reached
9,722,425-203	1.31	795	Air until RT is reached
9,712,182-204	1.51	795	Air until RT is reached
9,722,418-107	1.49	795	Air until RT is reached
9,722,417-205	1.33	895	Water until $T = 665$ °C and then in air to RT
9,722,417-255	1.33	895	Water until $T = 665$ °C and then in air to RT
9,722,416-205	1.31	895	Water until $T = 665$ °C and then in air to RT
9,722,416-255	1.31	895	Water until $T = 665$ °C and then in air to RT
9,722,425-204	1.53	895	Water until $T = 665$ °C and then in air to RT
9,712,174-106	1.48	895	Water until $T = 665$ °C and then in air to RT
9,712,182-206	1.51	895	Water until $T = 665$ °C and then in air to RT
9,722,418-104	1.49	895	Water until $T = 665$ °C and then in air to RT

(a) Initial rolling temperature for all rolling schedules was 1020 °C.

9,722,425) with high Mn contents (1.49, 1.51, and 1.53 wt%, respectively) was carried out. The final thickness of the sheet was ≈ 2.28 cm, which was achieved during 11 to 13 rolling steps. The final rolling temperature was ≈ 835 °C ($\alpha + \gamma$ region), and after the last rolling pass, the rolled plates were cooled in air. Details of cast and slab number are in Table 2.

Rolling schedule No. 2: A controlled rolling procedure for four slabs (9,722,416; 9,722,416; 9,722,425; and 9,722,417) with low Mn contents (1.31, 1.31, 1.31 and 1.33 wt%, respectively) and two slabs (9,722,418 and 9,712,182) with high Mn contents (1.49 and 1.51 wt%, respectively) was carried out. The final thickness was ≈ 2.28 cm, which was achieved during 11 to 15 rolling steps. The final rolling temperature was ≈ 795 °C ($\alpha + \gamma$ region). After the last rolling pass, the rolled plates were cooled in air.

Rolling schedule No. 3: A controlled rolling for four slabs (9,722,416; 9,722,416; 9,722,417; and 9,722,417) with low Mn contents (of 1.31, 1.31, 1.33, and 1.33 wt%, respectively) and for four slabs (9,712,174; 9,722,418; 9,712,182; and 9,722,425) with high Mn contents (1.48, 1.49, 1.51, and 1.53 wt%, respectively) was carried out. The final thickness was ≈ 2.28 cm, which was achieved with 11 to 15 rolling steps. The final rolling temperature was ≈ 895 °C ($\alpha + \gamma$ region). After the last rolling pass, the rolled plate was cooled by means of an accelerated process, so that the rolled plate was cooled from ≈ 895 °C ($\alpha + \gamma$ region) to ≈ 665 °C (α region) in an average time of 30 s, after which the plates were cooled in air.

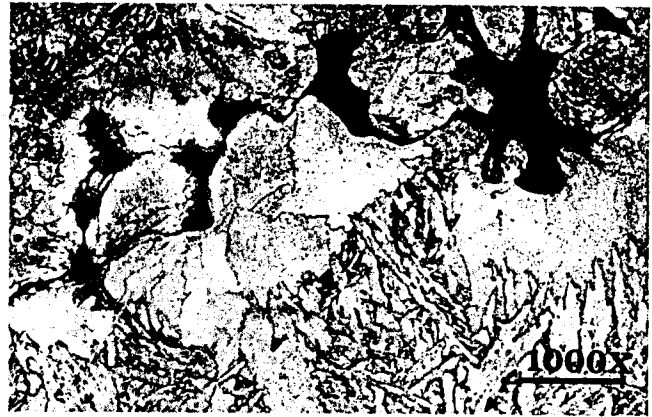
Microstructural characterization of slabs and sheets was carried out using an Olympus optical microscope (Olympus America Inc., Melville, NY), a stereoscan Leica 440 scanning electron microscope (SEM) (Leica Microsystems Inc., Deerfield, IL) and a Jeol 1200 transmission electron microscope (TEM) (Jeol de Mexico, S.A. de C.V, Hipodromo, Mexico). Preparation of samples for each stage was carried out by following established procedures. Hydrogen-induced cracking (HIC) tests on rolled sheets were carried out according to National Association of Corrosion Engineers (NACE) standard TM0284-96 method.

3. Results and Discussion

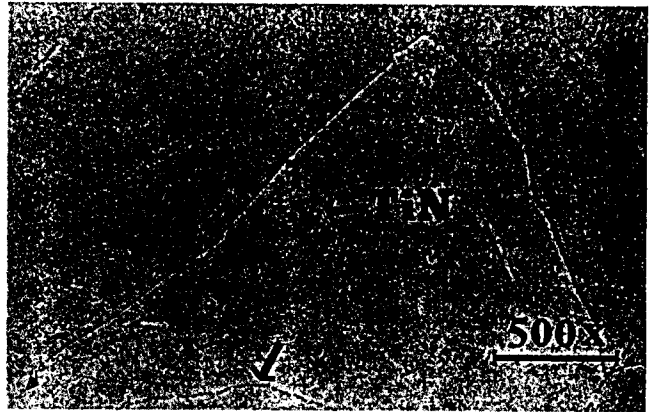
The observed as-cast microstructure positioned in the central region of the slab showed a centerline segregation region together with several small shrinkage holes. Inclusions were not detected in those regions (Fig. 1a). The area of segregation was not continuous and showed areas of about 0.0030 by 0.0033 m. The shrinkage holes were sized between 1×10^{-6} and 4×10^{-5} m distributed along a length of 0.08 m, with a separation between them of approximately 2×10^{-3} to 4×10^{-3} m. Scanning electron microscopic analysis carried out in the segregated region showed low amounts of segregated elements. For instance, the segregation ratio was about 1.055 for Mn, about 1.030 for Nb, and about 1.10 for chromium (Cr). The presence of MnS was not detected.

As has been pointed out (Ref 10), the solidification of low carbon steels starts with the nucleation and growth of δ -ferrite grains, as shown in Fig. 1(b) in which former δ -ferrite grain boundaries are decorated with precipitates. The precipitates

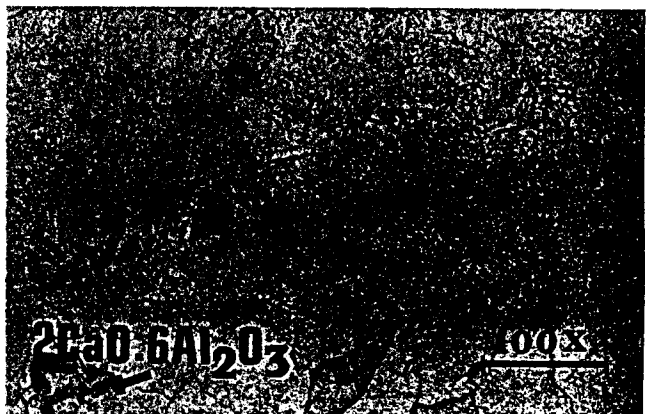
were identified by means of SEM analysis as titanium-rich carbides and niobium-rich carbides. Explanation of these has been presented elsewhere (Ref 11, 12). Shown also in Fig. 1 is the presence of a cuboidlike morphology, which was identified by means of SEM analysis as TiN precipitates located mainly in the ferritic matrix. Random spherical inclusions also were identified by means of SEM analysis as $2\text{CaO} \cdot 6\text{Al}_2\text{O}_3$, as shown in Fig. 1(c).



(a)



(b)



(c)

Fig. 1 As-cast microstructure. (a) Central region of the slab showing shrinkage holes. (b) Ti/Nb rich particles (shown by an arrow) in former δ -ferrite traces and TiN cuboidlike precipitates in ferritic matrix. (c) Random spherical inclusions of the $2\text{CaO} \cdot 6\text{Al}_2\text{O}_3$ type

The microstructure observed in slab specimens rolled according to schedule No. 1 consisted of deformed ferrite grains with the presence of few patches of pearlite. Inside the ferrite



(a)



(b)



(c)

Fig. 2 As-rolled microstructure (a) according to rolling schedule No. 1, showing ferritic grains with the presence of few patches of pearlite; (b) according to rolling schedule No 2, showing ferritic grains with very few patches of pearlite; and (c) according to rolling schedule No 3, showing ferritic grains with no patches of pearlite but areas of bainite (marked by several arrows). The single arrow shows nonmetallic inclusions of the $2\text{CaO}\cdot 6\text{Al}_2\text{O}_3$ type.

grains, the presence of precipitates associated with subgrain boundaries could be observed. Random inclusions of the $2\text{CaO}\cdot 6\text{Al}_2\text{O}_3$ type were detected (Fig. 2a). The microstructure observed in slab specimens rolled according to schedule No. 2 consisted once again of deformed ferritic grains with very few patches of pearlite. The presence of precipitates at subgrain boundaries was also observed. TiN precipitates were observed in the ferritic matrix, and inclusions of the $2\text{CaO}\cdot 6\text{Al}_2\text{O}_3$ type were also identified (Fig. 2b). Figure 2(c) shows the microstructure observed in the slab specimens rolled according to schedule No. 3 and consisting of deformed ferritic grains with an average grain size of $12 \pm 2 \mu\text{m}$. No patches of pearlite were detected, but some areas of bainite were observed. As in all the observed specimens, the presence of precipitates associated with subgrain boundaries was detected. These precipitates were identified by means of SEM microanalysis as Nb-rich carbides, and TiN precipitates were also observed in ferritic matrix. Spherical inclusions of the $2\text{CaO}\cdot 6\text{Al}_2\text{O}_3$ type were also detected. Microhardness Vickers measurements carried out in areas of ferrite grains showed values ranging from 210 to 229 kg/m^2 . Some regions (about 7% of the structure) reflect the presence of a bainitic microstructure (shown by an arrow). Microhardness Vickers measurements carried out in those bainitic regions showed values between 302 to 336 kg/m^2 .

Figure 3(a) shows TEM corresponding to a specimen that presented the mechanical properties equivalent to an API 5L X-70 grade steel. As shown, the presence of cubic and plate-shaped precipitate was observed. This precipitate was identified by means of its electron diffraction pattern (Fig. 3b) as TiN precipitate (with $a = 4.24 \text{ \AA}$) according to the following equation (Ref 13):

$$\log (\text{wt}\% \text{ Ti}) (\text{wt}\% \text{ N}) = -15,200/T + 3.9 \quad (\text{Eq 1})$$

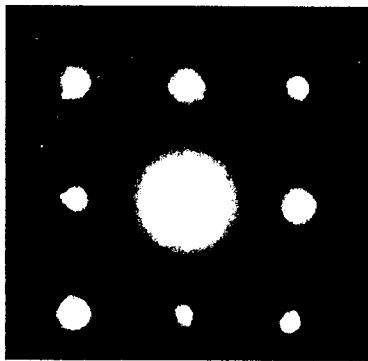
For the titanium and nitrogen concentration shown in Table 1, the temperature, T , needed for TiN precipitation is about 1840 °C, which confirms that TiN precipitation occurs at the liquid steel temperature. These TiN precipitates were sized up to 2 μm .

The presence of niobium carbides or carbonitrides was detected and is shown in Fig. 4(a). The lattice parameter of these niobium carbides or carbonitrides was determined by means of electron diffraction pattern as $a \approx 4.47 \text{ \AA}$ (Fig. 4b). According to Fig. 5 (Ref 14), which shows the niobium-carbonitride solubility curves in austenite, and taking the relationship of wt% C + 12 to 14 wt% N between 0.02 and 0.03, the carbonitrides in steels begin to precipitate at about 1075 °C for a Nb content in the range of 0.092 to 0.095 wt%. This precipitation occurred on the deformed austenite grains during the last stages of the rough rolling schedule. The particle size of these precipitates was in the range of 50 to 200 nm.

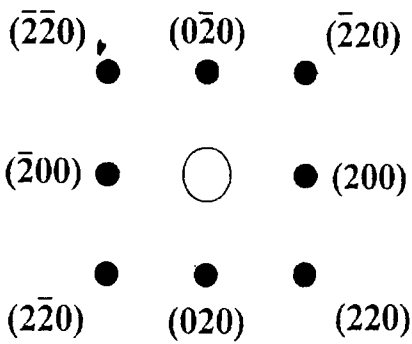
As a result of the microstructural characterization, it was observed that N was properly combined as nitrides. One of the first nitrides formed at high temperature is TiN, which reduces the negative effect of free nitrogen (harmful to toughness). Another purpose of adding Ti is to retard austenite recrystallization during austenite deformation, owing to the relatively large size of the solute atom.



(a)



(b)

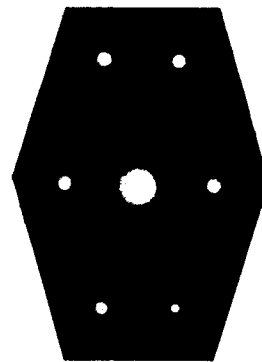


(c)

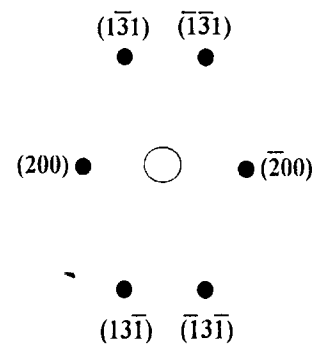
Fig. 3 (a) Transmission electron micrograph (TEM) corresponding to a specimen that presented mechanical properties equivalent to those of an API 5L X-70 steel. The arrow shows the presence of cuboidlike TiN precipitate. (b) Diffraction pattern of precipitates. (c) Key diagram for the diffraction pattern of precipitates



(a)



(b)



(c)

Fig. 4 (a) Transmission electron micrograph (TEM) corresponding to a specimen that presented mechanical properties equivalent to those of an API 5L X-70 steel. The arrow shows the presence of precipitates of the niobium carbonitride type. (b) Diffraction pattern of precipitates. (c) Key diagram for the diffraction pattern of precipitates

Table 3 Mechanical properties obtained in 20 plates from the experimental casts of steel grade API 5L X-70 from Imexsa

Cast	Mn, wt %	Rolling procedure	Average mechanical properties	
			Yield strength, ksi	Tensile strength, ksi
9,722,417-253	1.33	Controlled	67.0	72.6
9,722,416-252	1.31	Controlled	69.4	72.2
9,712,173-207	1.28	Controlled	68.5	73.0
9,722,425-253	1.53	Controlled	70.0	76.3
9,712,182-205	1.51	Controlled	67.2	73.2
9,722,418-109	1.49	Controlled	67.2	73.2
9,722,417-203	1.33	Controlled	69.6	74.3
9,722,416-202	1.31	Controlled	71.5	74.9
9,722,416-203	1.31	Controlled	74.0	76.6
9,722,425-203	1.31	Controlled	75.4	80.2
9,712,182-204	1.51	Controlled	72.0	76.4
9,722,418-107	1.49	Controlled	70.6	76.4
9,722,417-205	1.33	Controlled + accelerated cooling	73.5	81.7
9,722,417-255	1.33	Controlled + accelerated cooling	72.1	78.3
9,722,416-205	1.31	Controlled + accelerated cooling	73.1	79.7
9,722,416-255	1.31	Controlled + accelerated cooling	77.6	84.9
9,722,425-204	1.53	Controlled + accelerated cooling	75.3	85.3
9,712,174-106	1.48	Controlled + accelerated cooling	74.2	83.3
9,712,182-206	1.51	Controlled + accelerated cooling	76.3	84.2
9,722,418-104	1.49	Controlled + accelerated cooling	79.3	87.9

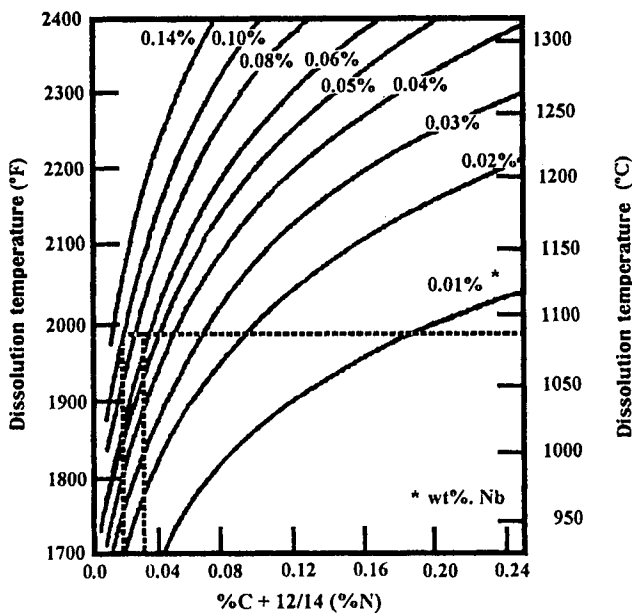


Fig. 5 Niobium-carbonitride solubility curves in austenite.
Source: Ref 14

Niobium (Nb) is another important element, because the amount of Ti present in the steel ensures that Nb remains in solid solution until a temperature of approximately 1075 °C is reached, so that Nb should precipitate. Precipitation of Nb as NbC or Nb(C, N) is useful because this maximizes grain refinement, which serves to improve both strength and toughness. This is one of the reasons for carrying out a controlled rolling procedure. Niobium is the most effective element in retarding recovery and recrystallization of deformed austenite. The presence of Nb will also produce a fine ferrite grain size and a greater volume fraction of bainitic transformation. The participation of vanadium (V) in this steel is to increase the strength levels due to the precipitation-hardening effect of V. Another

important element in the improvement of properties of this grade of steel is the Mn. For instance, at higher contents, Mn will improve toughness with equal levels of strength.

Finally, copper (Cu) is another element that is used for solid solution hardening. Apart from having this effect, Cu sometimes effectively prevents hydrogen formation.

After rolling of slabs, plates with thickness of about 2.28 cm were obtained. Several specimens were taken from the resulting plates in order to carry out tensile tests. From the tensile test results, Table 3 was obtained. According to Table 3, the rolling schedule that yielded the mechanical properties (determined in specimens cut in the transverse direction to the rolling one) equivalent to the steel grade API 5L X-70, in terms of yield strength (YS) (70 to 77 ksi of 0.2% YS) and tensile strength (TS) (82 ksi TS) corresponds to casts 9,722,416; 9,722,425; 9,722,174; 9,722,182; and 9,722,418. The processed slabs correspond to rolling practice No. 3, where the initial rolling temperature was 1020 °C and the final rolling temperature was 895 °C, followed by an accelerated cooling with an initial cooling temperature of 895 °C and a final cooling temperature of 665 °C (in 30 s) plus air cooling (except for the cast 9,722,425 that achieved the properties by using rolling schedules No. 2 and 3). Manganese contents are between 131 and 153 wt%.

One relevant outcome of this experimental trial from slabs is that the controlled rolling plus an accelerated cooling schedule produced an API 5L X-70 grade steel for large diameter pipes (36 in. in external diameter) with resistance to sour gas attack. In order to achieve the desired mechanical properties of the API 5L X-70 grade steel, the steelmaking route to obtain the desired chemical composition of the steel and the rolling procedure to obtain the desired microstructure and resultant mechanical properties must be taken into account. For instance, Fig. 6 shows a schematic representation of the thermomechanical controlled rolling schedule plus the effect of an accelerated cooling procedure in line. At the reheating temperatures of slabs (i.e., 1250 °C), the austenite grain size has a value between 100 and 200 μm. As the roughing rolling

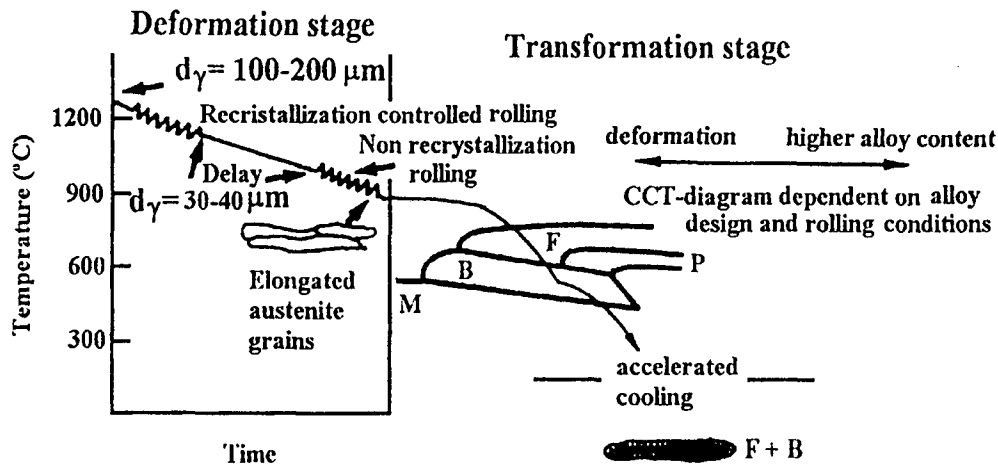


Fig. 6 Schematic representation of the thermomechanical controlled rolling and accelerated cooling procedure applied to API 5L X-70 slabs

procedures start, the grain recrystallizes, ending at temperatures above the Ar_3 temperature and finishing with a grain size in the range of 30 to 40 μm . Before the final rolling procedure starts, a delay permits starting the rolling procedure at the desired rolling temperature of the slabs in a nonrecrystallization range, with the aim of achieving an elongated austenite grain where the ferrite grain will nucleate. After this controlled rolling procedure, the cooling of plates plays an important role, because this cooling process produces the desired microstructure with its concomitant mechanical properties. For instance, in Fig. 6 it is shown (on the right hand side) that an accelerated cooling process immediately after the final rolling schedule produces a microstructure that can be of a ferrite/bainite type. Depending on the cooling media, a characteristic microstructure in the steel plate is obtained, which presents a different set of mechanical properties as compared to that obtained by using a classic air cooling procedure (ferrite or ferrite + pearlite).

4. Conclusions

- With respect to the steelmaking procedure adopted at Imexsa to obtain a cast with a chemical composition needed for the controlled rolling plus continuous cooling procedure to produce a sheet with the mechanical properties equivalent to an API 5L X-70 grade steel with resistance to sour gas attack, a chemical composition that fulfills that need can be traced from Table 3.
- The thermomechanical procedure to follow is that in which a final rolling step starts at a rolling temperature of 1020 °C, finishing at 895 °C, and followed by an accelerated cooling (about 6 °C/s) until a temperature of 660 °C is reached. Then, the sheet is left to cool in air, in order to achieve the mechanical properties of an API 5L X-70 grade.
- Steelmaking technology together with the controlled rolling plus accelerated cooling procedure applied to the steel ensures a steel of the API 5L X-70 grade with resistance to sour gas attack.

References

1. R. Mendoza, J. Camacho, G. Lugo, L. Herrera, J. Reyes, C. Gonzalez, and J.A. Juarez-Islas, Structure of Low Carbon Al-Killed/Ti-Added Steel, *ISIJ International*, Vol 37, 1997, p 176-180
2. K. Hulka, B. Bergmann, and A. Streibelberger, Development Trends in High Strength Structural Steels, *Proc. of the International Conf. on Processing, Microstructure and Properties of Microalloyed and Other Modern High Strength Low Alloy Steels*, A.J. DeArdo, Ed., The Iron and Steel Institute, 1991, p 177-187
3. K. Hulka, *Rolling and Alloying as Influencing Factors on Pipe Steel Properties, Specialty Steels and Hard Materials*, N.R. Comins and J.B. Clarck, Ed., Pergamon Press, 1983, p 267-276
4. T. Hashimoto and Y. Komizo, "Development of Low Pcm X70 Grade Line Pipe for Prevention of Cracking during Girth Welding, Welding in Energy-Related Project," Welding Institute of Canada, Toronto, 1983, p 63-71
5. K. Hulka, F. Heisterkamp, and I. I. Frantov, An Economic Approach to Pipe Steels with High Toughness and Good Weldability, *Pipeline Technology Conf. Proc.*, R. Denys, Ed., Antwerpen, Belgium, 1990, p 43-65
6. P.E. Repas, Metallurgical Fundamentals for HSLA Steels, *Microalloyed HSLA Steels '88*, ASM International, 1988, p 3-14
7. G.R. Speich, J.L. Cuddy, C.R. Gordon, and A.J. DeArdo, *Phase Transformations in Ferrous Alloys*, The Metallurgical Society of AIME, Warrendale, PA, 1984, p 341-389
8. R.S. Hostetter, H. Kranenberg, and J. Bathelt, *Fourth International Steel Rolling Conf.* (Deauville, France), 1987, p B2.1-B2.10
9. J.G. Williams, C.R. Killmore, J.F. Barret, and A.K. Church, *Processing, Microstructure, and Properties of HSLA Steels*, Metallurgical Society of AIME, Warrendale, PA, 1988
10. A.C. Kneissl, C.I. Garcia, and A.J. DeArdo, *Proc. of the International Conf. on Processing, Microstructure and Properties of Microalloyed and Other Modern High Strength Low Alloy Steels*, A.J. DeArdo, Ed., Pittsburgh, PA, 1991, p 145-152
11. J.L. Verger-Gaugry, G. Ocampo, and J.D. Embury, *Metallography*, Vol 18, 1985, p 381
12. R. Kleemaier, M. Michelitsch, A. Kneissl, and F. Jeglitsch, *Pract. Metallogr.*, Vol 26, 1989, p 248
13. K. Narita, *Trans. Iron Steel Inst. Jpn.*, Vol 15, 1975, p 147
14. K.J. Irvine, F.B. Pickering, and T. Gladman, *J. Iron Steel Inst.*, Vol 205, 1967, p 81-102